Z.Phys. C57 (1993) 595-604

DESY 92-135
October 92

ISSN 0418-9833

arXiv:hep-ph/9211305 v3 28 Nov 1992

Higher-Order QCD Corrections to Inclusive Particle Production in $p\bar{p}$ Collisions

F.M. Borzumati
B.A. Kniehl
G. Kramer

II. Institut für Theoretische Physik *
Universität Hamburg, 2000 Hamburg 50, Germany

Abstract

Inclusive single-particle production cross sections have been calculated including higher-order QCD corrections. Transverse-momentum and rapidity distributions are presented and the scale dependence is studied. The results are compared with experimental data from the CERN Sp$\bar{p}$S Collider and the Fermilab Tevatron.

*Supported by the Bundesministerium für Forschung und Technologie, 05 5HH 91P(8), Bonn, FRG.

1 Introduction

The inclusive production of single hadrons in hadronic collisions has long been recognized as an important process for testing the QCD-improved parton model (for reviews on the subject see, for instance, ref. [1]). The leading-order (LO) QCD formalism consists of using the tree-level results for the hard cross sections, the one-loop expression for the running coupling constant, and parton densities (structure functions) and fragmentation functions generated by one-loop evolution kernels. This theory provides a rather consistent description of many large-momentum-transfer processes [2]. The tree-level parton-parton scattering cross sections that enter this formalism have been calculated many years ago and an extensive phenomenology has been developed and confronted with experimental data [3, 4].

First results for next-to-leading order (NLO) corrections to hard-scattering processes have been obtained by Ellis et al. [5] in 1980. However, these authors considered only subprocesses with quarks in the initial state. Using quark distribution functions defined in deep inelastic scattering and fragmentation functions defined in one-particle inclusive e^+e^- annihilation, they found large corrections. Meanwhile, a complete NLO calculation involving all parton-parton processes contributing to hadron-hadron collisions has been presented by Aversa at al. [6].

These results are requisite in order to perform a consistent calculation of single-hadron production in the NLO formalism. This involves NLO hard-scattering cross sections with two-loop α_S, two-loop-evolved structure functions and fragmentation functions. Only under these circumstances are all four elements unambiguously defined. Using NLO results for hard-scattering cross sections, structure and fragmentation functions in combination, should reduce substantially the scale dependence of the predictions for inclusive one-particle cross sections, since the variation in one of these factors is compensated by the others up to still missing higher-order terms. To guarantee this compensation, a consistent choice of renormalization and factorization schemes and scales is necessary in all four elements entering the analysis. As mentioned above, NLO results for all parton-parton subprocesses are available.

As is well known, structure and fragmentation functions cannot be calculated yet from the QCD Lagrangian. For their construction one has to resort to experimental data, in particular from total inclusive deep-inelastic lepton-nucleon scattering in the case of the structure functions and from one-particle inclusive e^+e^- annihilation in the case of the fragmentation functions. As for structure functions, such analyses based on NLO evolution and all existing data have been carried out by several groups, even including processes other than deep-inelastic lepton-nucleon scattering [7, 8]; for a recent review see [9].

Unfortunately, such analyses do not exist for the fragmentation functions of quarks and gluons. Although the relevant NLO theory is well known [10] and inclusive single-particle distributions of various hadrons have been measured in e^+e^- annihilation as well as in semi-inclusive deep-inelastic lepton-nucleon scattering, such a NLO analysis has not been tackled yet. All the existing information on fragmentation functions is based on

LO evolution equations and also on rather old data [4, 11]. Although this represents a serious limitation to any NLO prediction of one-particle production in hadron-hadron, photon-hadron, or lepton-hadron reactions, we consider it appropriate to make the first step and to combine the available results for the NLO parton-parton hard-scattering cross sections and the NLO parton distribution functions to obtain more reliable predictions as compared with the LO theory considered in the past.

Inclusive single-hadron production provides both advantages and disadvantages as compared to jet production. A distinct hadron constitutes a final state which is better defined than a jet event, since the latter delicately depends on the details of the jet-finding algorithm. Moreover, the definition of a jet becomes more problematic at low energy. On the other hand, the fragmentation of the produced parton renders the p_T distributions quite steep and reduces therefore the range experimentally accessible in the case of single-hadron production. Accordingly, the experimental errors are large in the high-p_{T} range, where the cross sections become considerably small, while the bulk of the data is accumulated at lower values of p_{T}.

In this paper we shall present cross sections for single-charged-hadron and single-π^0 production in $p\bar{p}$ reactions. Similar predictions for γp and low-Q^2 ep processes will be considered in a separate communication. Experimental data for charged one-particle and π^0 production at relatively low centre-of-mass (CM) energies come from the CERN ISR pp Collider [12]. At higher energies, data from the UA1 [13] and UA2 [14] Collaborations at the Sp$\bar{\mathrm{p}}$S Collider and from the CDF Collaboration [15] at the Tevatron are available. Since the QCD-improved parton model should work best for the $p\bar{p}$ collider energy range, we shall compare our results with data for the higher energies only. Specifically, we choose data at $\sqrt{s} = 540$ and 630 GeV from UA2 and CDF, respectively and at 1.8 TeV from CDF.

The outline of this paper is as follows. In Sect. 2, we give a short introduction of the formalism and fix our notation and input. Results of our calculation are presented in Sects. 3 and 4, where we also compare with data from $p\bar{p}$ colliders. Sect. 5 is reserved for a discussion of the results and some concluding remarks.

2 Formalism, Notation, and Input

In the LO QCD-improved parton model the single-particle cross section can be expressed as a convolution of the LO parton-parton scattering cross sections with the scale-dependent structure and fragmentation functions. We fix the momenta of the hadron reaction by

$$h_1(p_1) + h_2(p_2) \to h_3(p_3) + X\,, \tag{1}$$

where h_1 and h_2 are the incoming hadrons and h_3 is the single hadron in the final state. In LO the cross section is given by

$$E_3 \frac{d^3\sigma^0}{d^3p_3} = \sum_{i,j,l} \int dx_1 \int dx_2 \int \frac{dx_3}{x_3^2}\; F_i^{h_1}(x_1, M^2)\, F_j^{h_2}(x_2, M^2)\, D_l^{h_3}\left(x_3, M_f^2\right)\; p_3^0 \frac{d^3\sigma^0_{k_i k_j \to k_l}}{d^3p_3} \tag{2}$$

where the partonic momenta k_i, k_j and k_l are expressed in terms of p_1, p_2 and p_3 as:

$$k_i = x_1 p_1, \quad k_j = x_2 p_2, \quad k_l = p_3/x_3\,.$$

The indices i, j, l run over gluons and N_F flavours of quarks. We assume $N_F = 4$ throughout our calculation and neglect the influence of the charm-quark threshold. $F_i^h(x, M^2)$ and $D_l^h(x, M_f^2)$ are the usual structure and fragmentation functions appropriate to partons of type i or l inside hadron h, which depend on the scales M and M_f to be specified later. Finally, $d^3\sigma^0_{k_i k_j \to k_l}$ characterizes the process $i + j \to l + X$ in $\mathcal{O}\left(\alpha_{\mathrm{S}}^2(\mu^2)\right)$.

Thus, we have three scales altogether: M, the factorization scale of the parton distributions F_i^h, M_f, the factorization scale of the fragmentation functions D_l^h, and μ, the renormalization scale of the QCD coupling constant α_{S}. In LO all three scales are left undefined. Usually they are linked to the transverse momentum p_{T} of the produced hadron h_3. Since this choice of scale is rather arbitrary, there is a large uncertainty of the theoretical predictions at the LO level.

In NLO the inclusive cross section is written as[†]

$$E_3 \frac{d^3\sigma^0}{d^3p_3} = \sum_{i,j,l} \int dx_1 \int dx_2 \int \frac{dx_3}{x_3^2}\, F_i^{h_1}(x_1, M^2) F_j^{h_2}(x_2, M^2) D_l^{h_3}\left(x_3, M_f^2\right) \times \left[\frac{1}{v}\left(\frac{d\sigma^0_{k_i k_j \to k_l}(s, v)}{dv}\right)\delta(1-w) + \frac{\alpha_{\mathrm{S}}(\mu^2)}{2\pi} K_{k_i k_j \to k_l}\left(s, v, w; \mu^2, M^2, M_f^2\right)\right], \tag{3}$$

where v and w can be expressed in term of the partonic variables s, t and u as:

$$v = 1 + t/s\,, \qquad w = -u/(s+t)\,.$$

[†] In the following, we largely follow the notation of Aversa et al. [6].

In turn, s, t and u are related to the hadronic variables $S = (p_1 + p_2)^2$, $T = (p_1 - p_3)^2$ and $U = (p_2 - p_3)^2$ by:

$$s = x_1 x_2 S\,, \qquad t = \frac{x_1}{x_3}\,T\,, \qquad u = \frac{x_2}{x_3}\,U\,,$$

The factors $K_{k_i k_j \to k_l}\left(s, v, w; \mu^2, M^2, M_f^2\right)$ are the NLO corrections.

The calculation of the correction terms $K_{k_i k_j \to k_l}$ is fully described in [6]. It is based on the results of Ellis and Sexton [16] for the matrix elements squared for all $(2 \to 2)$ and $(2 \to 3)$ parton scattering subprocesses calculated to $\mathcal{O}\left(\alpha_{\rm S}^3\right)$. The $K_{k_i k_j \to k_l}$ functions are plagued by infrared and collinear divergences, which appear as poles in the parameter $\varepsilon = (4 - n)/2$, with n being the dimensionality of space-time. The cancellation of the infrared singularities, which are $\propto 1/\varepsilon^2$, is explained in [6]. The left-over $1/\varepsilon$ singularities associated with ingoing parton lines are absorbed into the bare distribution functions $F_i^h(x)$, which renders them dependent on the scale M. Similarly, the $1/\varepsilon$ singularities from outgoing parton lines are absorbed into the bare fragmentation functions $D_l^h(x)$, so that they become dependent on the scale M_f.

After all these cancellations and absorptions have been done, the single-hadron inclusive cross section has the form (3) with the correction terms $K_{k_i k_j \to k_l}$ being given by [6]

$$\begin{aligned} K_{k_i k_j \to k_l}&\left(s, v, w; \mu^2, M^2, M_f^2\right) = \\ &\frac{1}{v}\left(\frac{d\sigma^0_{k_i k_j \to k_l}(s,v)}{dv}\right) \quad \left\{\left(c_1 + \tilde{c}_1 \ln\frac{s}{M^2} + \tilde{\tilde{c}}_1 \ln\frac{s}{M_f^2} + \hat{c}_1 \ln\frac{s}{\mu^2}\right)\delta(1-w)\right. \\ &\qquad + \left(c_2 + \tilde{c}_2 \ln\frac{s}{M^2} + \tilde{\tilde{c}}_2 \ln\frac{s}{M_f^2}\right)\left(\frac{1}{1-w}\right)_+ + c_3\left[\frac{\ln(1-w)}{1-w}\right]_+\Bigg\} \\ &\qquad\qquad + K'_{k_i k_j \to k_l}(s, v, w)\,, \end{aligned} \tag{4}$$

where the $K'_{k_i k_j \to k_l}(s, v, w)$ functions are regular in the limit $w \to 1$. The coefficients c_i, $\tilde{c}_i$, $\tilde{\tilde{c}}_i$, and $\hat{c}_i$ may be found in [6] for the various subprocesses. The $K'_{k_i k_j \to k_l}$ functions are given by rather lengthy expressions and have been communicated to us by the authors of [6].

The form of the various coefficients and the $K'_{k_i k_j \to k_l}$ functions in (4) depend on the choice of the finite corrections $f_{ij}(x)$ and $d_{ij}(x)$ $(i, j = q, g)$ to structure and fragmentation functions. These finite corrections have to be adjusted according to the selected factorization scheme. The authors of [6] advocate a scheme where all f_{ij} and d_{ij} are kept different from zero in the form specified in [6]. However, this alternative reaches beyond the scope of present structure-function analyses, since it affects higher orders relative to the NLO level, and we shall not follow it. The popular DIS and $\overline{\rm MS}$ schemes require $f_{ij} = d_{ij} = 0$, except for f_{qq} and d_{qq}, which are finite and different for the two schemes. The expressions for f_{qq} and d_{qq} listed in [6] correspond to structure and fragmentation functions in the $\overline{\rm MS}$ scheme. Since fragmentation functions have been determined only to LO, the $\overline{\rm MS}$ scheme

is appropriate here ($d_{qq} \neq 0$). As for structure functions, results are available in both $\overline{\rm MS}$ and DIS schemes. Depending on the choice of scheme, the appropriate forms of f_{qq} must be selected in the NLO corrections to the parton-level cross sections.

As already mentioned in the introduction, we shall employ the fragmentation functions by Baier et al. [4] and Anselmino et al. [11], which appears to be the best choice for the time being. Reference [11] provides us with functions for the fragmentation of u and d quarks into $\pi^\pm$ and $K^\pm$ as a function of the scale M_f. They are obtained from fits to EMC deep-inelastic lepton scattering data. We adopt the fragmentation functions of the gluon into $\pi^{\pm,0}$ from [4], with $D_g^{\pi^+} = D_g^{\pi^-} = D_g^{\pi^0}$. These, as well as the u and d quark fragmentation functions have a reference scale $Q_0 = 5\,\mathrm{GeV}$. Following [17], we identify the fragmentation function of the s quark into a given pion with the one of the first-family quark that is not a ground-state constituent of the respective pion, e.g., $D_s^{\pi^+} = D_d^{\pi^+}$, etc. We proceed similarly in the case of c quarks. The fragmentation functions into kaons emerge from those into pions through multiplication by heuristic reduction factors [11].

The proton structure function parametrizations used in our calculcations are taken from the package by K. Charchuła [18]. For the central results and, in particular, for the comparison with experimental data we use the Morfin-Tung set MT-B1 [7], either in the DIS or in the $\overline{\rm MS}$ version.

In the next sections, we shall present our results in two steps. In the first step, we assume $D_i^h(x_3, M_f^2) = \delta(1 - x_3)$ for all hadrons h and partons i. In this way, we study the cross sections for the production of single partons. Although these cross sections cannot be compared with experimental data—a fragmentation function $\sim \delta(1 - x_3)$ is a reasonable approximation only for heavy quarks—, they are simpler to calculate and reveal several features and dependences that are also relevant for the complete single-hadron cross sections considered in the second step. We emphasize that these cross sections must not be compared with experimental jet production cross sections, since they lack a recombination algorithm indispensable for defining jets.

3 Results: Single-Parton Inclusive Cross Section

In this section we approximate all fragmentation functions by δ functions. This leads to single-parton inclusive cross sections. For a first orientation, we disentangle the various parton-parton channels that contribute in LO to the hard-scattering cross section, viz.

1) $gg \to gg$,

2) $gg \to q\bar{q}$,

3) $gq \to gq, qg$ and $qg \to qg, gq$,

4) $q\bar{q} \to gg$,

5) $qq \to qq$,

6) $q\bar{q} \to q\bar{q}, \bar{q}q$,

7) $q\bar{q} \to q'\bar{q}'$,

8) $qq' \to qq', q'q$,

where q and q' denote different quark flavours. In Fig. 1, this is done for $d\sigma/dp_{\mathrm{T}}$ at $\sqrt{s} = 630\,\mathrm{GeV}$ using the LO set SL of the Morfin-Tung structure functions [7]. Here and in the following figure we choose $\mu = M = p_{\mathrm{T}}$. We observe that at small p_{T} the two channels 1) and 3) dominate by more than one order of magnitude, whereas at larger p_{T} ($p_{\mathrm{T}} > 30\,\mathrm{GeV}$) also the pure quark channels 6) and 8) contribute significantly. Similar observations have been made in the past [19]. It is clear that the magnitude of the cross sections with gluonic initial states are highly sensitive to the gluon content of the proton (antiproton), whose small-x behaviour is still not well known. Of course, the relative size of the various channels in Fig. 1 is subject to change when realistic fragmentation functions are taken into account.

Next, we study how our results are influenced when different sets of structure functions are used. Toward this end, we calculate $d^3\sigma/dy\,d^2p_{\mathrm{T}}$ in the Born approximation at $\sqrt{s} = 630\,\mathrm{GeV}$ and $y = 0$ as a function of p_{T} using in turn the structure-function sets MT-B1 (DIS), MT-B1 ($\overline{\mathrm{MS}}$) [7] and MRSn-D0 ($\overline{\mathrm{MS}}$), MRSn-D$-$ ($\overline{\mathrm{MS}}$) [20], which are all NLO structure functions. For the QCD coupling α_{S} we employ the usual one-loop formula. In Fig. 2, we show these cross sections normalized with respect to the value obtained when the MT-SL set is used. Strictly speaking, only the latter should be combined with the LO hard-scattering cross sections because it is a genuine LO fit; all the others correspond to NLO analyses of present data.

We observe that the variation caused by replacing the LO set by the various NLO sets does not exceed some 30% for $p_{\mathrm{T}} > 5\,\mathrm{GeV}$. The DIS and $\overline{\mathrm{MS}}$ versions of MT-B1 differ by only 10% relative to each other. We may consider this as an upper bound on the scheme dependence, since the partial compensation that is expected to take place at NLO due

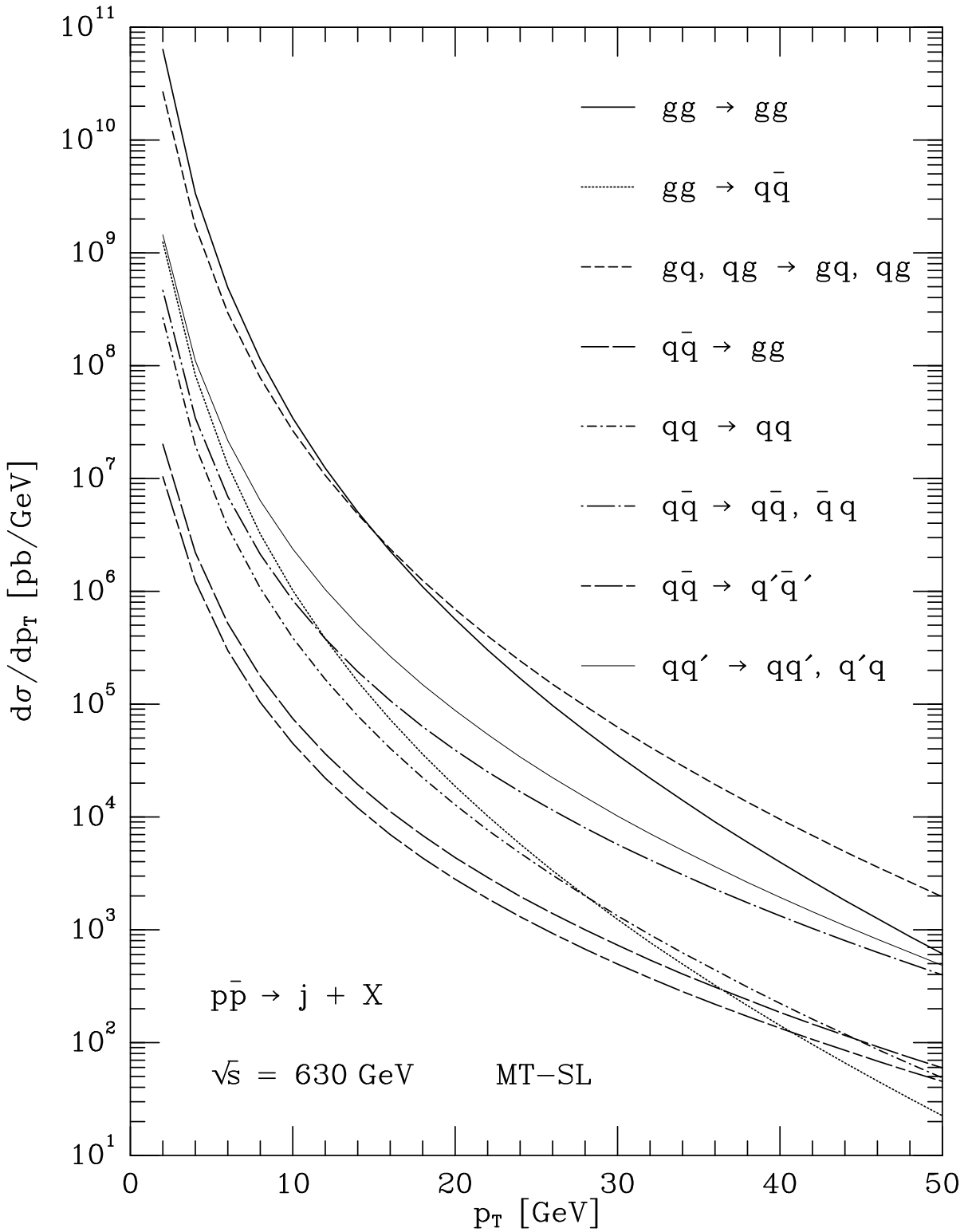

Figure 1: p_{T} distributions of the various LO channels at $\sqrt{s} = 630\,\mathrm{GeV}$ evaluated with the LO set SL of the Morfin-Tung structure functions.

Figure 2: Influence of typical NLO structure functions on the LO calculation of $d^3\sigma/dy\,d^2p_T$ at $\sqrt{s} = 630\,\mathrm{GeV}$ and $y = 0$. The curves are normalized to the LO calculation with the MT-SL set.

to scheme-dependent terms is not in effect here. The MRSn-D0 and MRSn-D$-$ fit also recent NMC and CCFR [21] data which extend to smaller values of x than previously tested. The results differ significantly at low p_T. In particular, the D0 and D$-$ sets differ drastically from each other. This may be understood by recalling that the gluon-initiated subprocesses dominate at low p_T; see Fig. 1. The variation is considerably reduced at larger p_T ($p_\mathrm{T} > 30\,\mathrm{GeV}$), where also the channels (6) and (8) contribute significantly. These features are expected to survive at NLO.

To investigate the influence of the higher-order terms in the hard-scattering cross sections, we calculate $d^3\sigma/dy\,d^2p_\mathrm{T}$ at $\sqrt{s} = 630\,\mathrm{GeV}$ and $y = 0$ as a function of $2p_\mathrm{T}/\sqrt{s}$ with and without these terms and plot the ratio in Fig. 3. In both numerator and denominator we use the same structure functions, namely the DIS or $\overline{\mathrm{MS}}$ versions of MT-B1, and the two-loop expression for α_S. The renormalization scale Λ of α_S is adjusted according to the structure functions. We do this for the three choices $\mu = M = M_f = p_\mathrm{T}/2$, p_T, and $2p_\mathrm{T}$. From Fig. 3 we see that this ratio is independent of p_T, except for small p_T. Its value ranges between 1.3 and 2.1, which demonstrates the importance of the NLO corrections to the parton-level cross sections. The scheme dependence DIS versus

Figure 3: $d^3\sigma/dy\,d^2p_T$ in NLO normalized to the corresponding calculation with the NLO terms in the hard-scattering cross sections omitted, for $\sqrt{s} = 630\,\mathrm{GeV}$, $y = 0$, and scales set to $p_\mathrm{T}/2$, p_T, and $2p_\mathrm{T}$. DIS and $\overline{\mathrm{MS}}$ results are compared.

$\overline{\mathrm{MS}}$ is negligible. Note that, in contrast to Fig. 2, the same structure functions are used in both numerator and denominator, so that variations due to changes of scheme or set largely cancel out. On the other hand, we observe a strong scale dependence, which is mainly due to the denominator as will become apparent below.

The scale dependence of numerator and denominator of the ratio considered in Fig. 3 is explicitly studied in Fig. 4a and 4b for p_T fixed at 31.5 GeV and 94.5 GeV, respectively. We set the three scales μ, M and M_f equal to ξp_T and we let ξ vary between 0.125 and 8. The higher values of ξ in Fig. 4b allow for scales exceeding the CM energy. For the results obtained in these figures, the DIS scheme is adopted in connection with the appropriate MT-B1 set. Obviously, the LO cross section (dashed line) exhibits a stronger dependence on the scale factor ξ as compared to the NLO result (solid line). The more rapid decrease of the LO cross section for increasing ξ explains the mild increase of the ratio plotted in Fig. 3. The NLO cross section is particularly insensitive to ξ for $\xi > 1$. This holds true independently of p_T, although the absolute cross section strongly varies with p_T; the cross sections shown in Figs. 4a and b differ by four orders of magnitude. The scale variation of the NLO cross section is well bounded in contrast to the LO cross

Figure 4: Scale dependence of $d^3\sigma/dy\,d^2p_T$ for $\sqrt{s} = 630\,\mathrm{GeV}$, $y = 0$, and a) $p_\mathrm{T} = 31.5\,\mathrm{GeV}$, b) $p_\mathrm{T} = 94.5\,\mathrm{GeV}$. The solid and dot-dashed lines represent the NLO results with variable and fixed M_f, respectively; the dashed lines represent the LO result with NLO structure functions and α_S.

section, which decreases monotonically with increasing ξ. However, one should keep in mind that the M_f dependence of the NLO result is not compensated as long as δ-function-type fragmentation is assumed. In this somewhat pathological situation it would be more appropriate not to vary M_f. For comparison, we have included the respective results in Fig. 4 also (dot-dashed curves).

4 Results: Single-Hadron Inclusive Cross Section.

In this section we shall present our results for the inclusive production of charged hadrons and of single π^0's. For the calculation of these cross sections we have employed the fragmentation functions already mentioned in Sect. 2. For the comparison with experimental data we have chosen the structure function MT-B1 in the DIS scheme. Collider data for charged hadrons ($h = (h^+ + h^-)/2$) come from the UA2 and CDF Collaborations [14, 15].

In Fig. 5 we compare the charged-hadron inclusive cross section as measured by UA2 at $\sqrt{s} = 540\,\mathrm{GeV}$, for $1.0 < y < 1.8$, with the results we obtain when the three different scales μ, M and M_f are simultaneously set equal to $p_\mathrm{T}/2$, p_T and $2p_\mathrm{T}$. This scale dependence is rather moderate and we shall discuss later on how it compares with the scale dependence in the LO cross section. Up to this uncertainty, this is an absolute prediction of the cross section. We observe that the prediction with scales equal to p_T is in adequate overall agreement with the data for p_T up to 10 GeV. The agreement is less satisfactory at small p_T, where higher order corrections may be appreciable. In addition, somewhere in this region non-perturbative effects come in.

Similar conclusions can be drawn for the comparisons shown in Figs. 6 and 7 with CDF data at $\sqrt{s} = 630\,\mathrm{GeV}$ and $\sqrt{s} = 1.8\,\mathrm{TeV}$, respectively. In both cases, the rapidity is averaged over the interval $-1 < y < 1$. The 1.8 TeV data at large p_T are again predicted best with scales equal to p_T. The same seems to be true for the 630 GeV data, although the p_T range is in this case too small to allow a firm statement.

Looking at the energy dependence, we note that $\sqrt{s}$ increases by a factor 3 as we go from Figs. 5,6 to Fig. 7. We observe that at small p_T, below 3 GeV, the cross section is independent of $\sqrt{s}$, whereas in the large-p_T range the cross section increases with increasing energy, i.e. it shows the characteristic flattening of the p_T distribution originating from the hard-scattering cross section. This behaviour of the data is borne out by the theory quite well although at small p_T we would not expect such a good agreement.

In order to get an idea of the size of the NLO correction in the hard scattering terms, we compare in Figs. 8, 9 and 10 the Born cross section with the NLO one for $\sqrt{s} = 540, 630\,\mathrm{GeV}$ and 1.8 TeV. Here, again, the cross sections are averaged over the rapidity ranges in the same way as for the respective experimental data. In the Born cross section the structure functions as well as the value of α_S are the same as in the NLO cross section. The effect of the NLO terms leads to an average K factor of approximately 1.5 for the choice of scales $\mu = M_f = M = p_\mathrm{T}$. For comparison, we show also the experimental data.

It has to be emphasized that this K factor is only a measure of the NLO corrections to the hard scattering. Usually one takes the attitude of comparing the NLO cross section to the LO one where the hard scattering, the structure functions and the strong coupling constant α_S are evaluated in lowest order. Such a K factor, denoted as *full/"born"*, is presented in Fig. 11a for the three scales $p_\mathrm{T}/2, p_\mathrm{T}$ and $2p_\mathrm{T}$, CM energy $\sqrt{s} = 1.8\,\mathrm{TeV}$ and $|y| < 1.0$. The parametrization MT-SL is used for the structure functions entering in the LO cross section. The value of 144 MeV for the QCD parameter Λ required by this parametrization is extended also to the α_S coupling constant and to the fragmentation

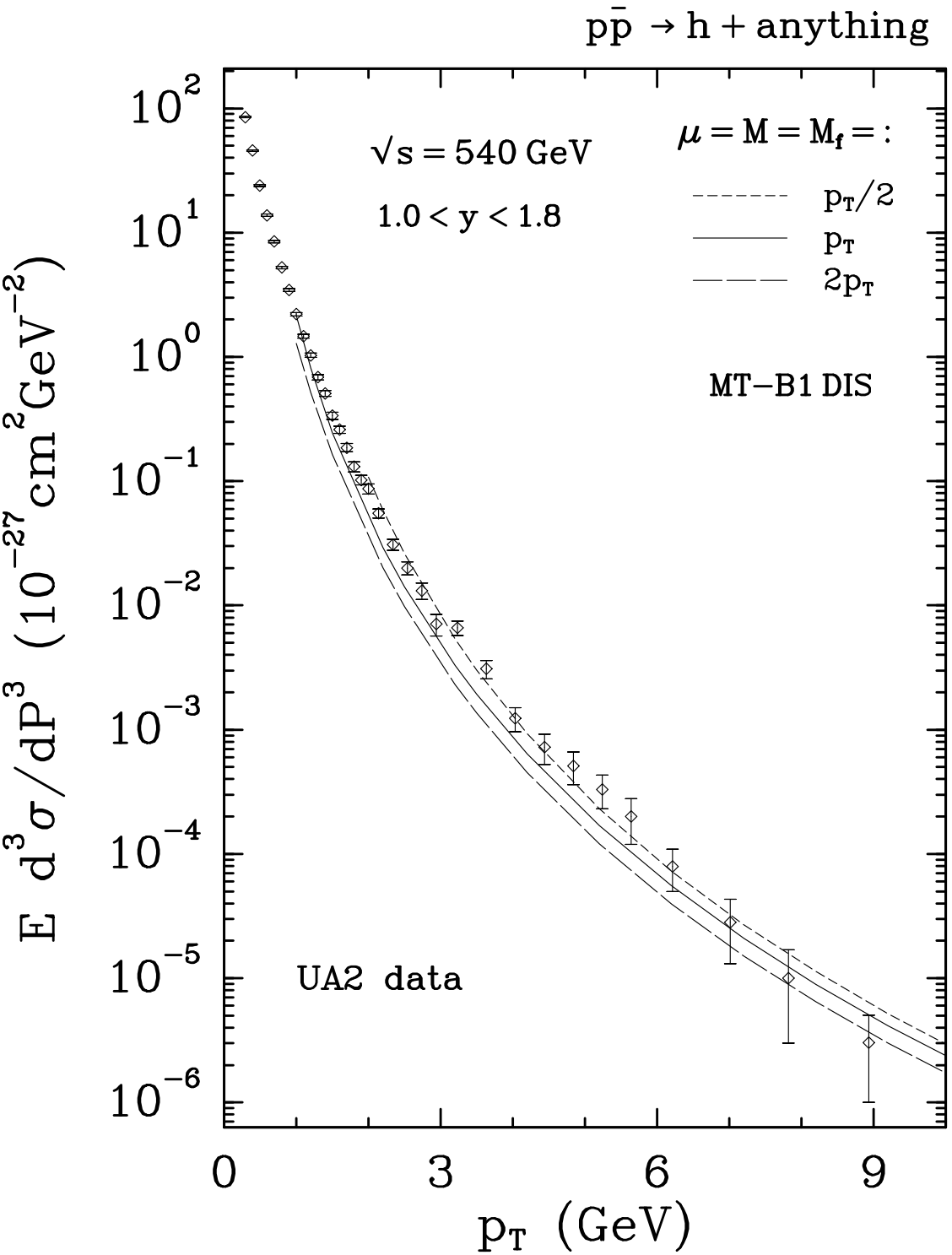

Figure 5: Inclusive charged-hadron production cross section for $\sqrt{s} = 540$ GeV, averaged over the rapidity range $1.0 < y < 1.8$. The short-dashed, solid and long-dashed lines correspond to the full NLO predictions for scales μ, M and M_f simultaneously set equal to $p_T/2$, p_T and $2p_T$. For comparison, the UA2 data taken at the same CM energy and in the same rapidity range are also shown.

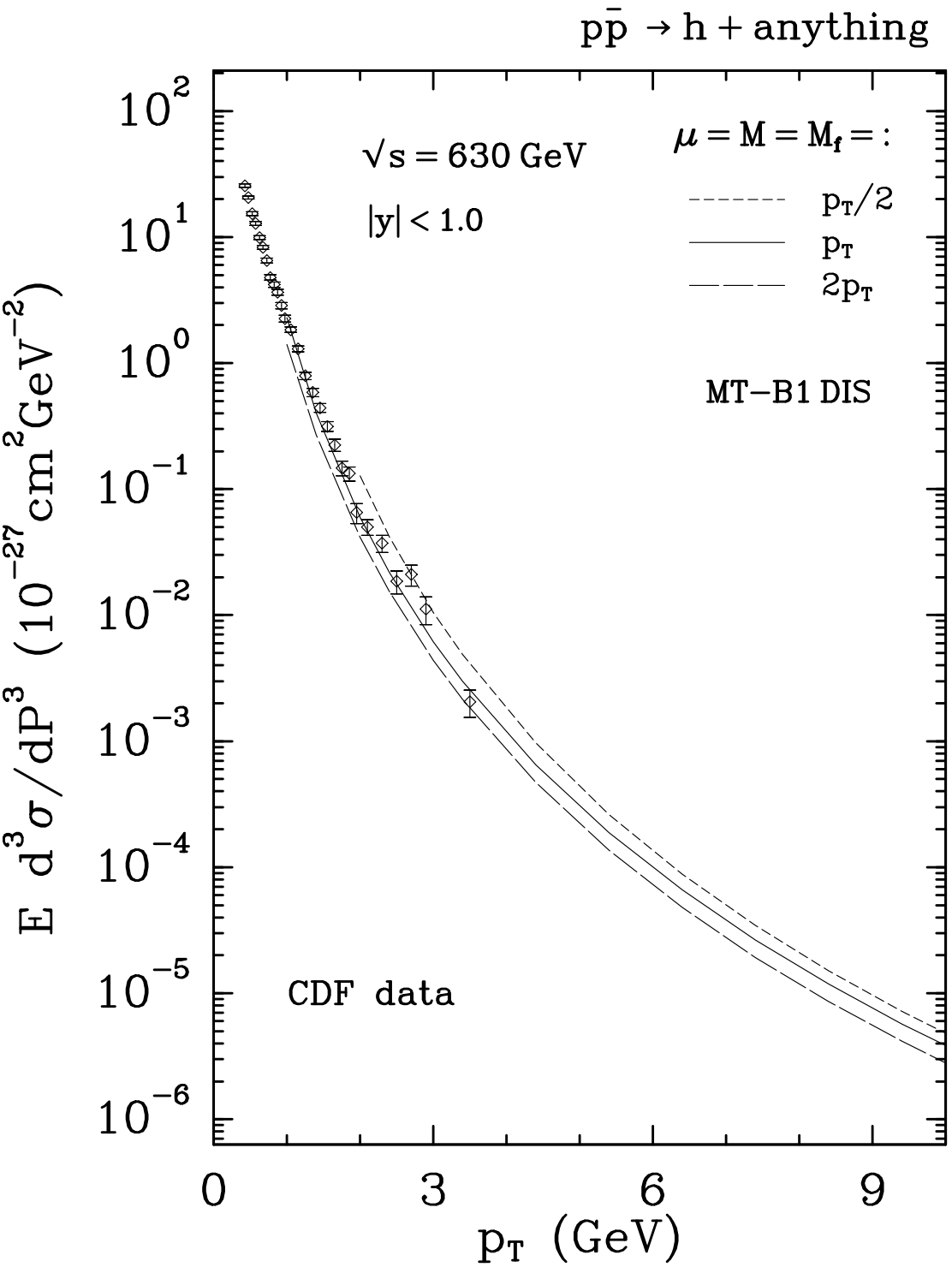

Figure 6: Same as in Fig. 5 for $\sqrt{s} = 630\,\mathrm{GeV}$ and rapidity range $|y| < 1.0$. The theoretical results are here compared with data obtained by the CDF Collaboration.

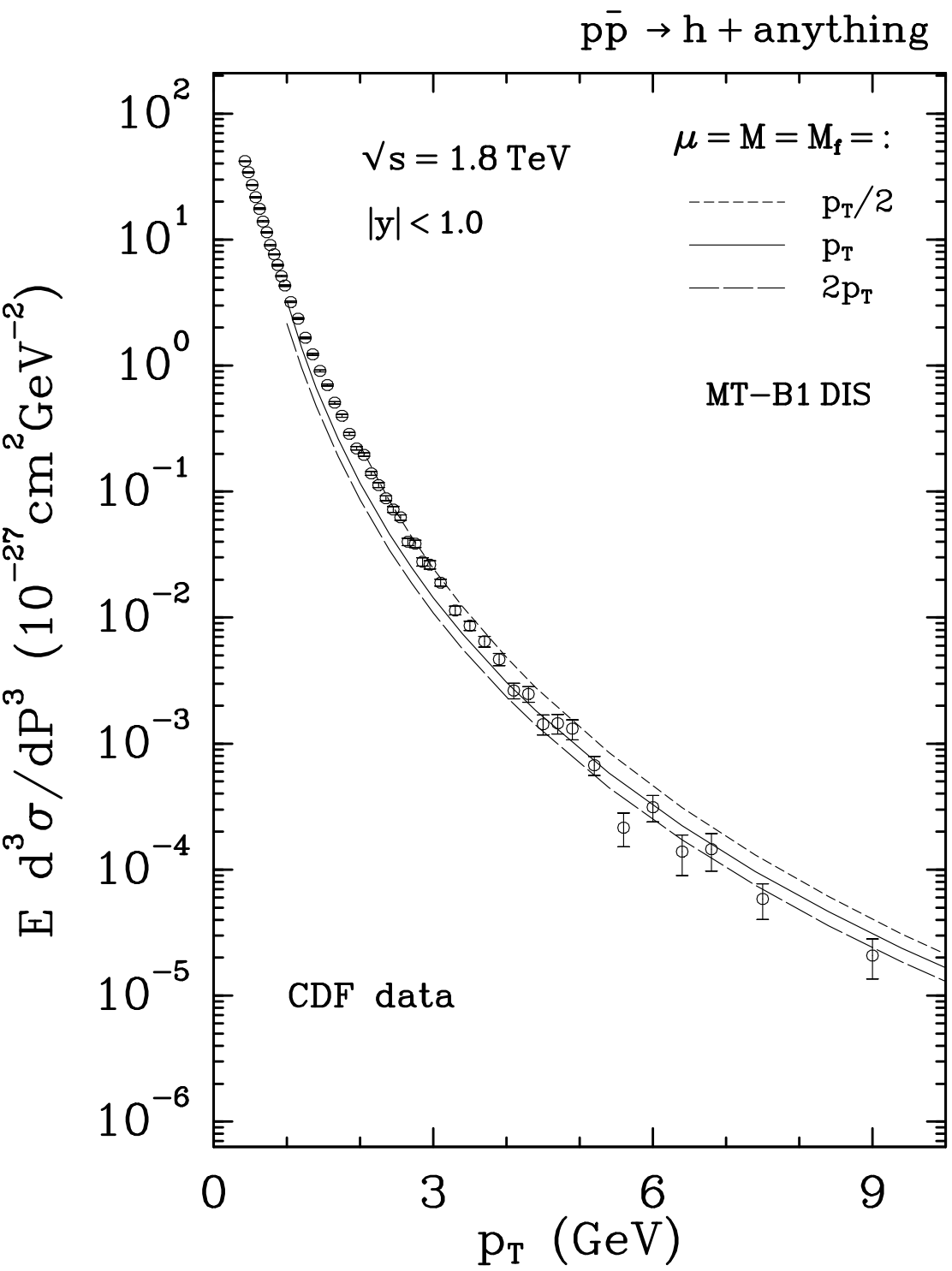

Figure 7: Same as in Fig. 6 for $\sqrt{s} = 1.8$ TeV.

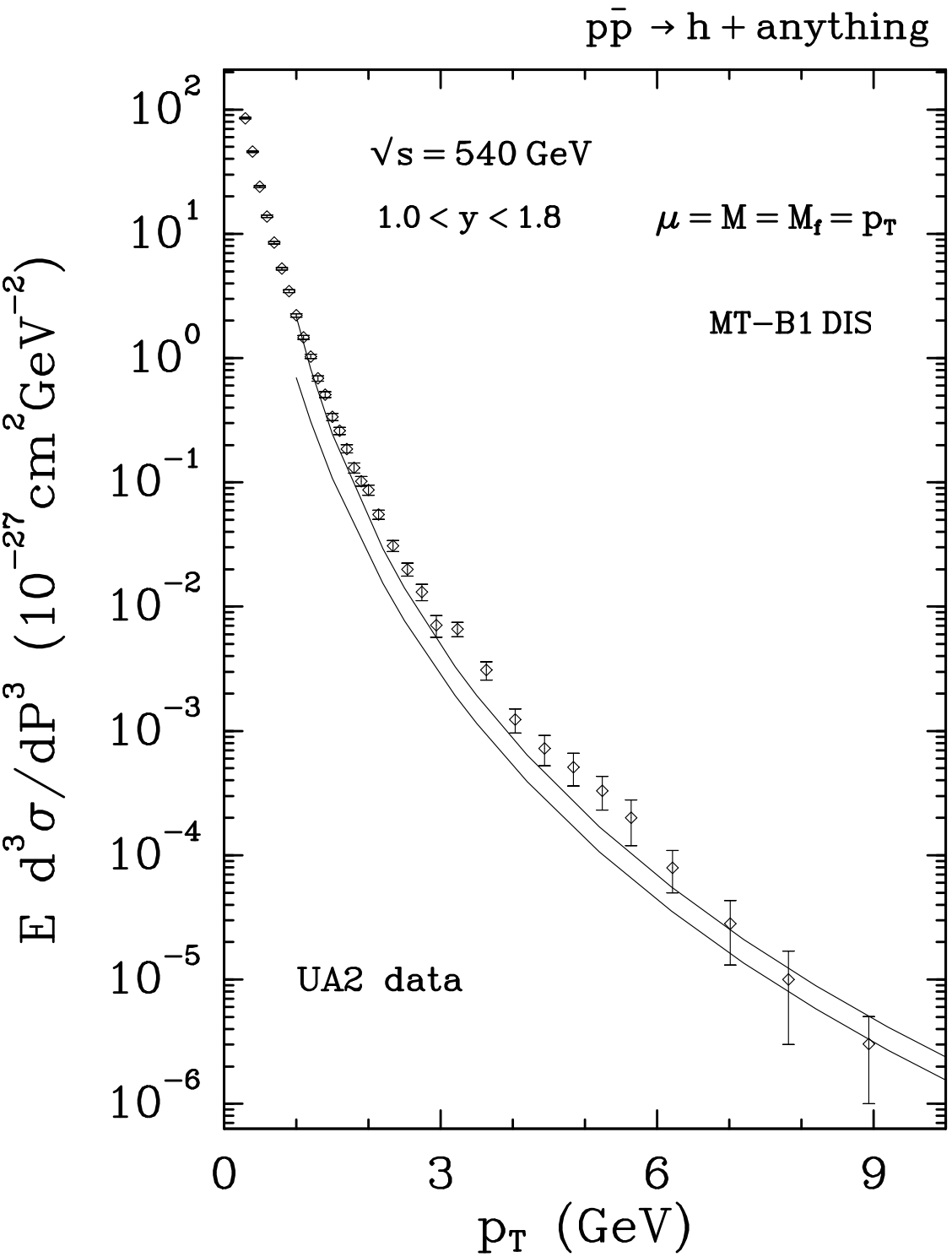

Figure 8: The experimental data shown in Fig. 5 are here compared to the NLO theoretical result (upper curve) and the LO one (lower curve) as obtained for structure functions and α_S kept at the NLO level.

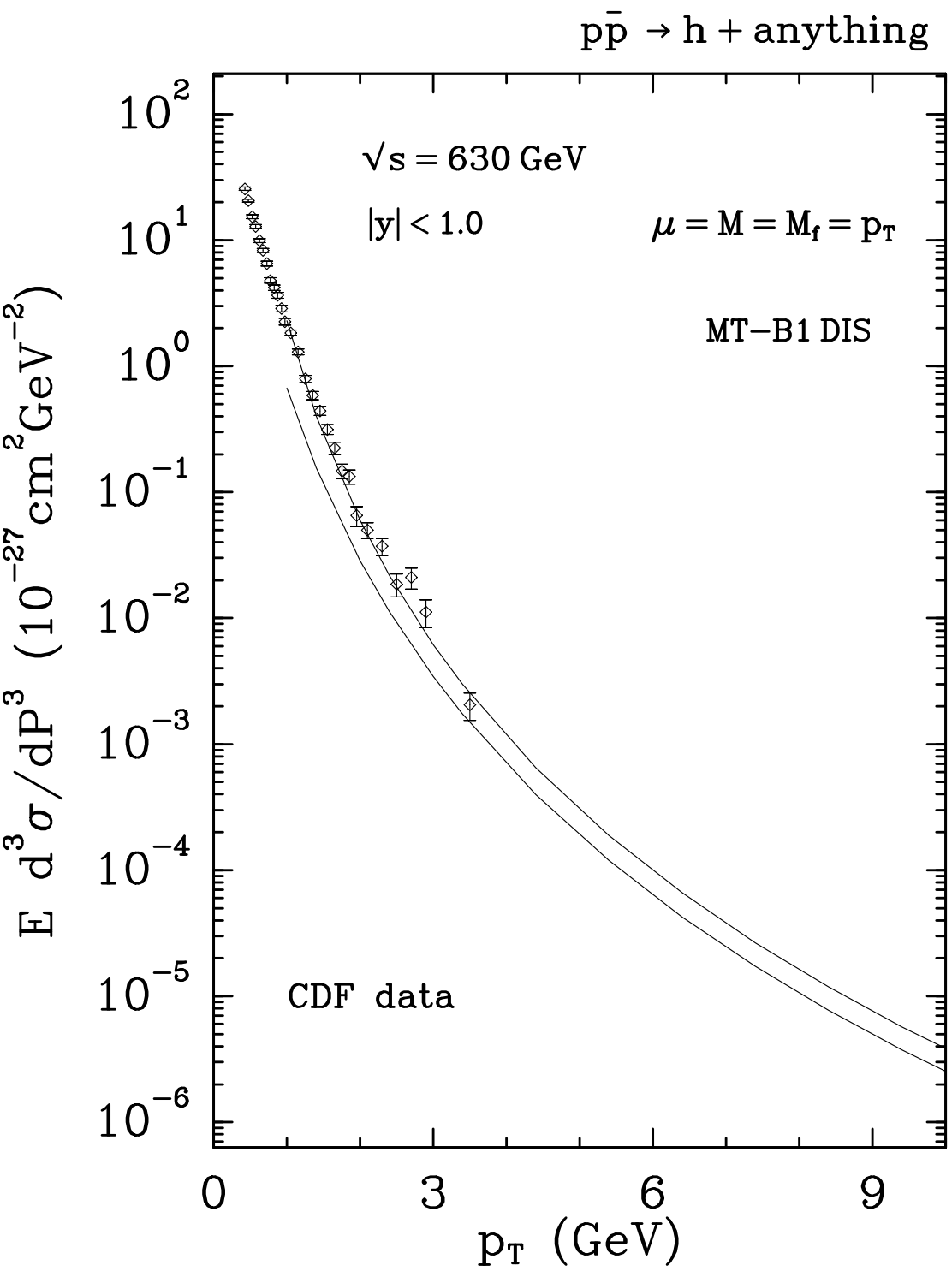

Figure 9: Same as in Fig. 8 for the data shown in Fig. 6.

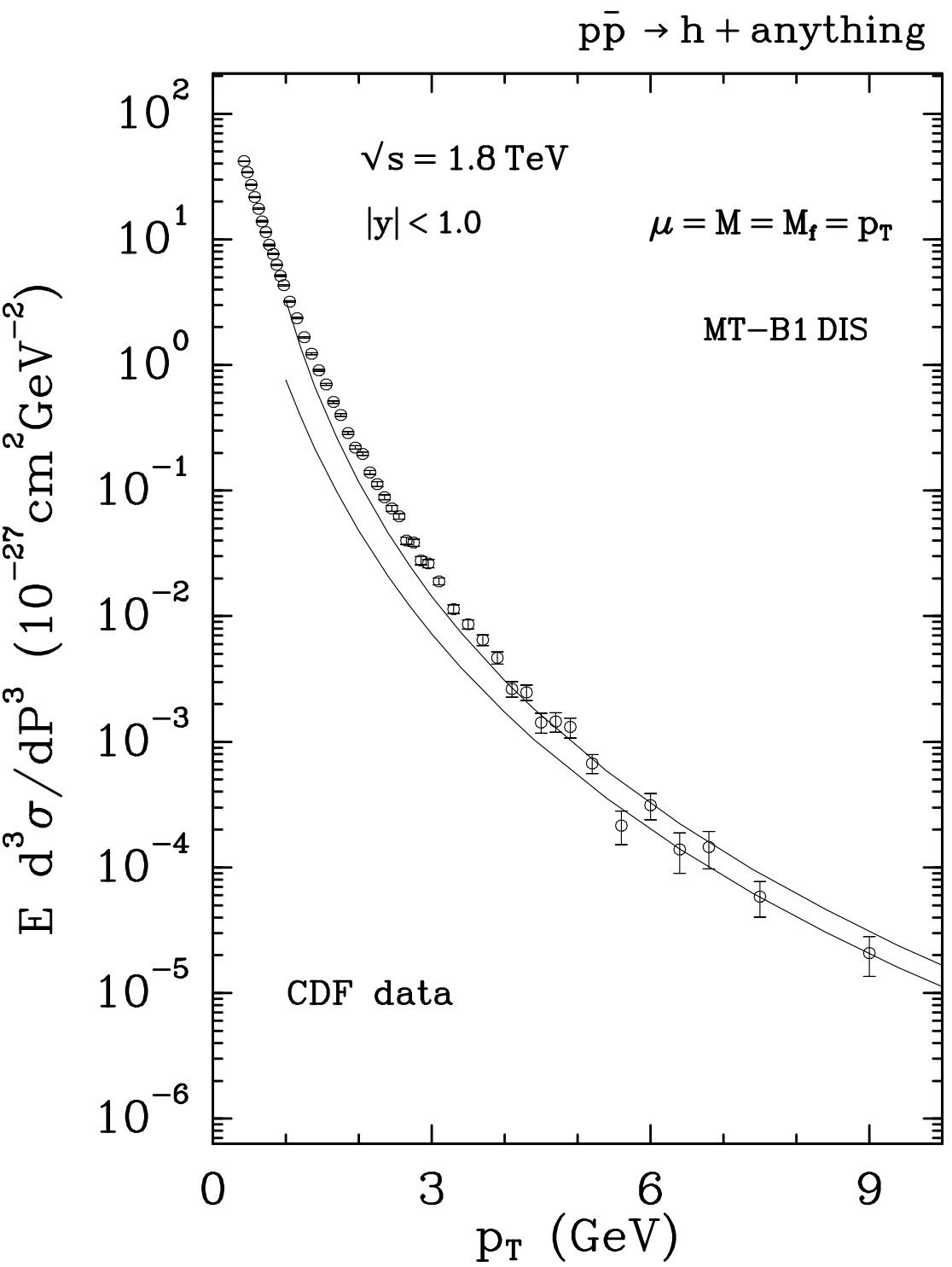

Figure 10: Same as in Fig. 8 for the data shown in Fig. 7.

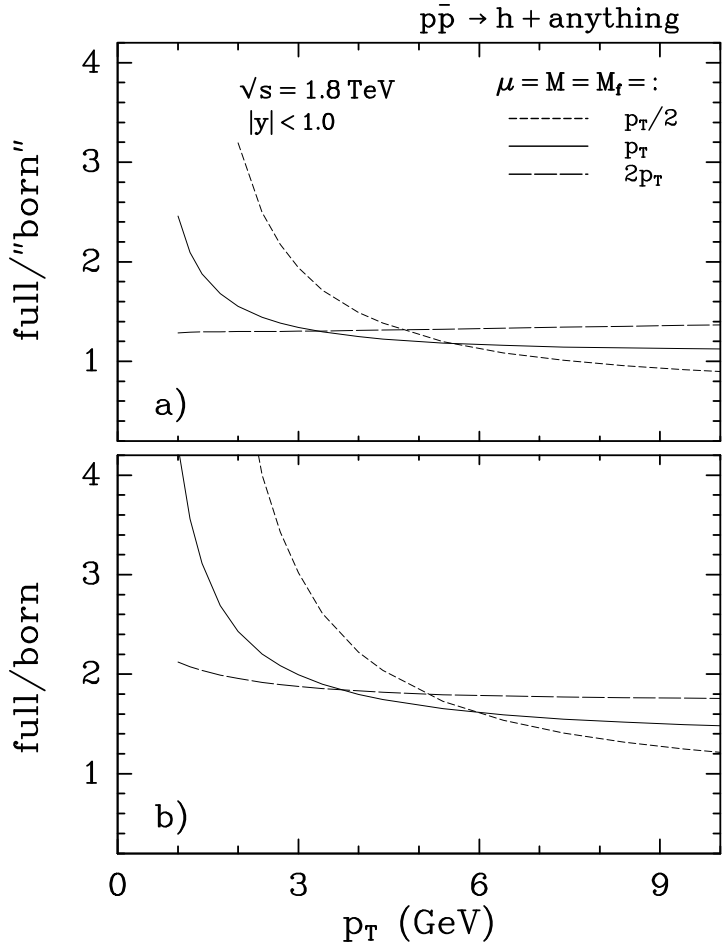

Figure 11: Ratios of the NLO charged-hadron production cross section over a) the LO one and b) the LO one evaluated with NLO structure functions and α_S, for $\sqrt{s} = 1.8\,\text{TeV}$, rapidity range $|y| < 1.0$ and scales equal to $p_T/2$, p_T and $2p_T$.

functions. We observe in Fig. 11a that the K factor obtained in this way is ~ 1 and almost p_T-independent for $p_T > 5\,\text{GeV}$ if the three scales μ, M and M_f are set equal to p_T. For the other two scales, $p_T/2$ and $2p_T$, the K factor has a somewhat stronger p_T dependence and reaches 0.9 and 1.4, respectively, for the higher values of p_T, where experimental data are available.

The K factor with structure functions and α_S kept at the NLO level, referred to above (*full/born*), is shown in Fig. 11b also for the same choices of scales. It is larger than the one shown in Fig. 11a, ranging between 1.2 and 1.8 at the upper end of the p_T-range studied here, and exhibits also a stronger scale and p_T dependence. We have verified that similar features are present also at $\sqrt{s} = 540$ and $630\,\text{GeV}$. K factors between 1 and 2 are obtained in these cases for scales varying between $p_T/2$ and $2p_T$, for $5\,\text{GeV} < p_T < 10\,\text{GeV}$. A weaker p_T dependence is observed at these lower CM energies: the ratios *full/born* are in these cases essentially flat for $p_T > 5\,\text{GeV}$ as also appears in Fig. 3, where δ-function fragmentation functions are assumed.

It is clear from these figures that if one goes from a *bona fide* LO theory to a NLO

combination of hard-scattering cross sections, structure functions and α_S, a strong compensation between these NLO effects takes place. On the other hand, less compensation is present when the NLO effects are contained only in the hard scattering. The importance of including the NLO corrections consistently in all components, as already emphasized by many authors (see for example [9]), is therefore quite evident.

To obtain more information on the scale dependence of the inclusive cross section, we have calculated it as a function of the scale factor ξ defined above for $p_T = 5, 10$ and 30 GeV, for CM energy $\sqrt{s} = 630$ GeV and rapidity range $|y| < 1.0$. Results are shown in Fig. 12 for the LO cross section (with LO structure function and α_S), for the NLO cross section and for a LO cross section with the same structure functions and α_S used in the NLO calculation.

We see quite clearly that the NLO cross section has much less scale dependence than the two LO ones. The NLO cross section develops a plateau at small values of ξ, for not-too-small p_T, i.e. $p_T > 5$ GeV. The large turn-over of this plateau, however, is presumably an artifact due to the use of LO fragmentation functions. For all p_T, both LO curves show a monotonic dependence on ξ. Between $\xi = 1$ and $\xi = 8$ the decrease of these two curves is steeper than the one shown by the NLO cross section. We also observe that the LO cross section (dotted curve) equals the NLO cross section for all three p_T at $\xi \approx 0.7$, whereas at larger values of ξ the two curves are quite well separated. This scale, where the true LO and the NLO results match, is advocated as the best possible choice of scales by the method of Fastest Apparent Convergence [22].

At this point, we should compare Fig. 12 for $p_T = 30$ GeV with Fig. 4a, where the scale dependence has been investigated at $\sqrt{s} = 630$ GeV and $p_T = 31.5$ GeV in the case of δ-function fragmentation. We notice that, apart from the absolute size, the LO results exhibit roughly the same qualitative features, which can be attributed to a rather weak scale dependence of the fragmentation functions. However, the situation changes appreciably when NLO corrections are included. Then, in the case of realistic fragmentation the cross section falls off less steeply at large ξ, due to compensations between the M_f dependence of the fragmentation functions and the M_f dependence of the hard-scattering cross sections. Finally, the drop-off at small ξ, when present, is also more pronounced in Fig. 12.

So far we have concentrated on the discussion of p_T distributions with rapidity integrated over a finite region. In Fig. 13 we show the differential cross section $d^3\sigma/d^2p_T dy$ as a function of the rapidity y for CM energy $\sqrt{s} = 630$ GeV and three different values of p_T: $p_T = 5, 10$ and 30 GeV. We observe that the NLO corrections to the hard-scattering cross section do not change the shape of this distribution. The full NLO cross section and the LO one both exhibit the same symmetric behaviour in y.

At last, we show the results we obtain on inclusive π^0 production at $\sqrt{s} = 540$ GeV for $1.0 < y < 1.8$ (Fig. 14) and $|y| < 0.6$, compared with the UA2 data taken at the same CM energy and in the same regions of rapidity (Fig. 15). It turns out that the data cannot be explained in NLO by using p_T as scale, unlike the case of inclusive charged-hadron production. Both choices of scales $\mu = M = M_f = p_T$ and $2p_T$ give cross sections

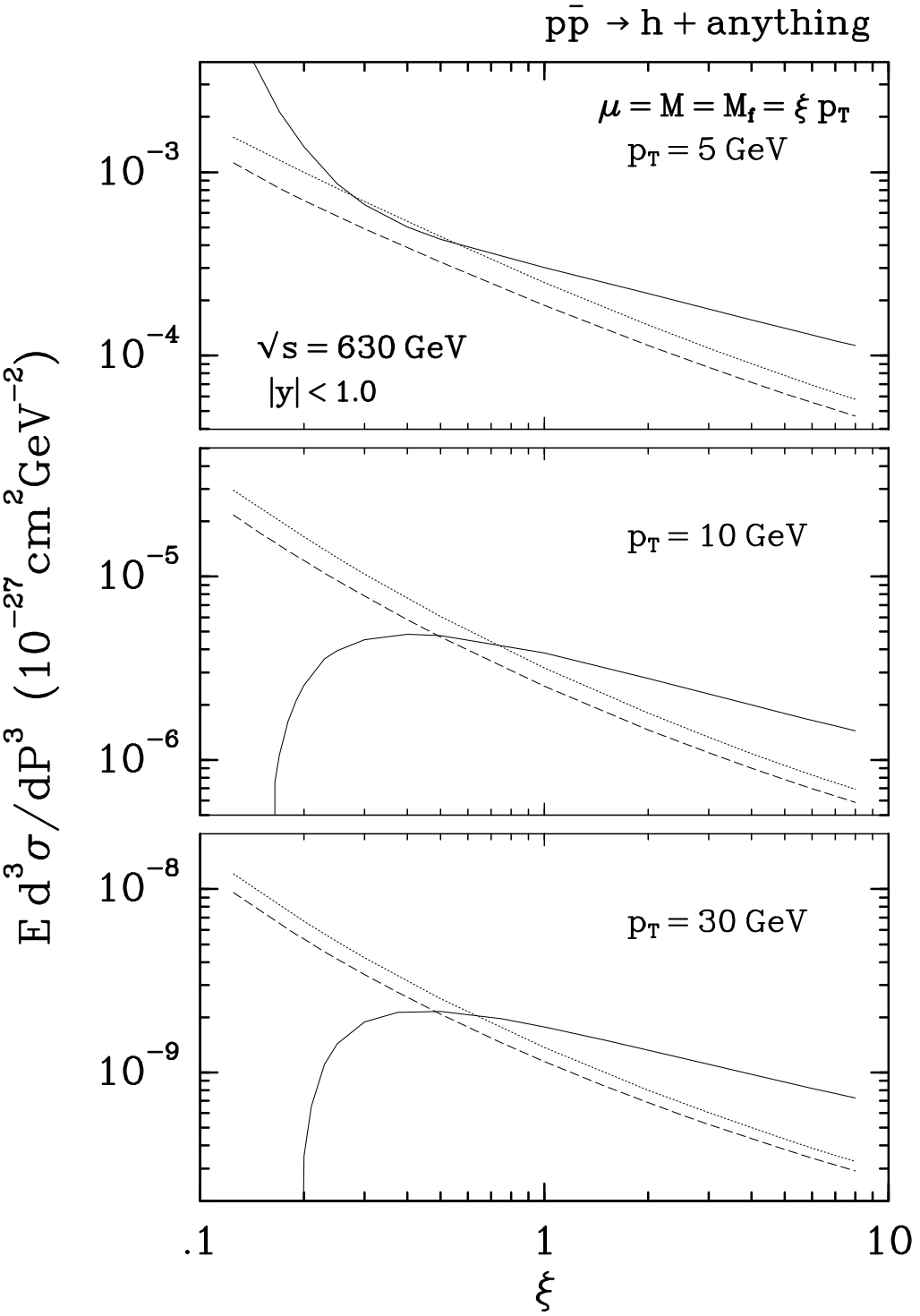

Figure 12: Scale dependence of the charged-hadron production cross section for $\sqrt{s} = 630\,\mathrm{GeV}$, $|y| < 1.0$ and $p_\mathrm{T} = 5, 10$ and $30\,\mathrm{GeV}$. The solid lines show the scale dependence of the NLO cross section. The dotted and dashed lines show the behaviour of the *bona fide* LO cross section and the LO one with NLO structure functions and α_S, respectively.

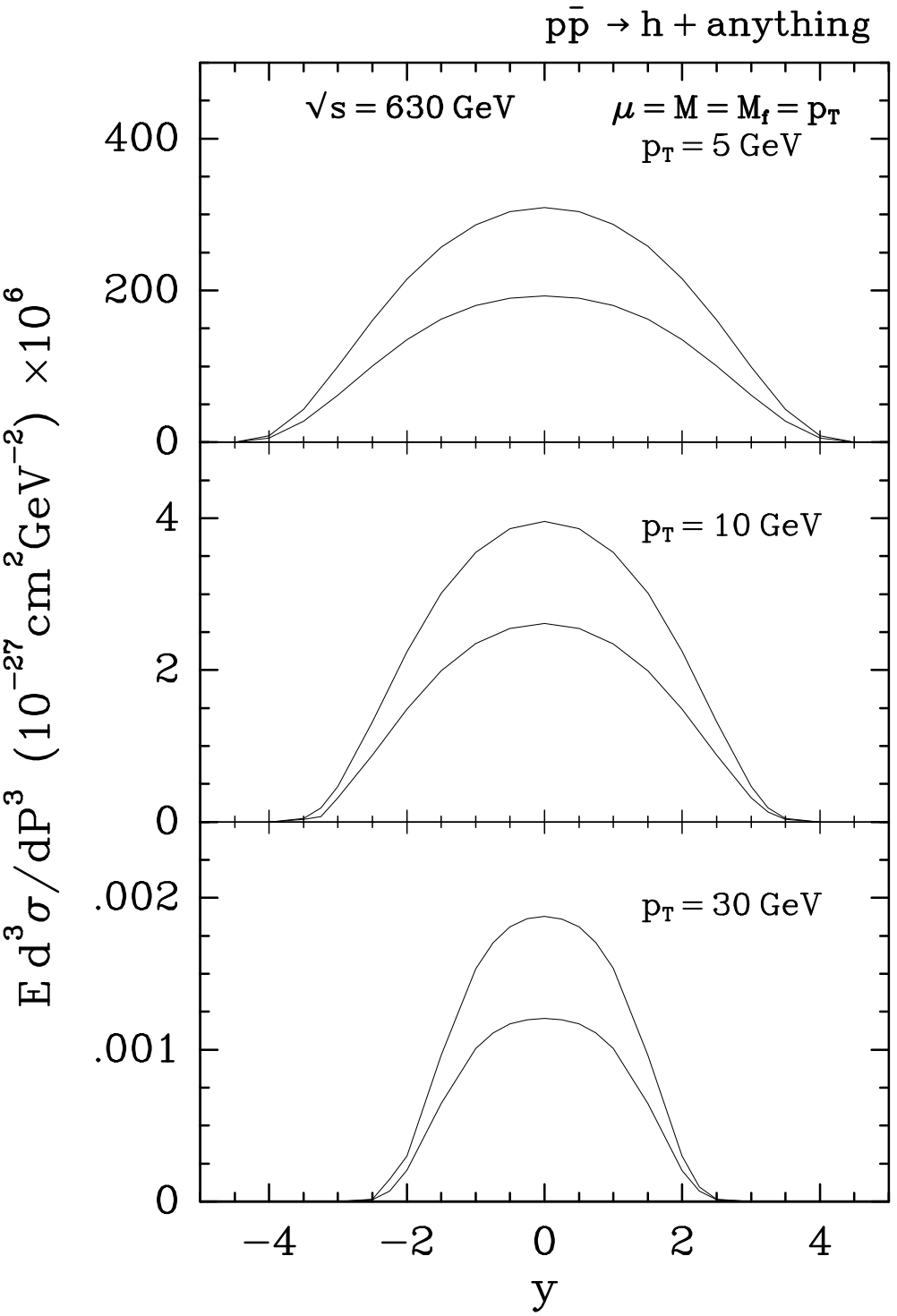

Figure 13: Rapidity distribution of the charged-hadron production cross section at $\sqrt{s} = 630\,\mathrm{GeV}$, scales fixed to p_T, for $p_\mathrm{T} = 5, 10$ and $30\,\mathrm{GeV}$. The upper curves show the y shape of the NLO cross section, the lower curves the shape of the LO one with structure functions and α_S at the NLO level.

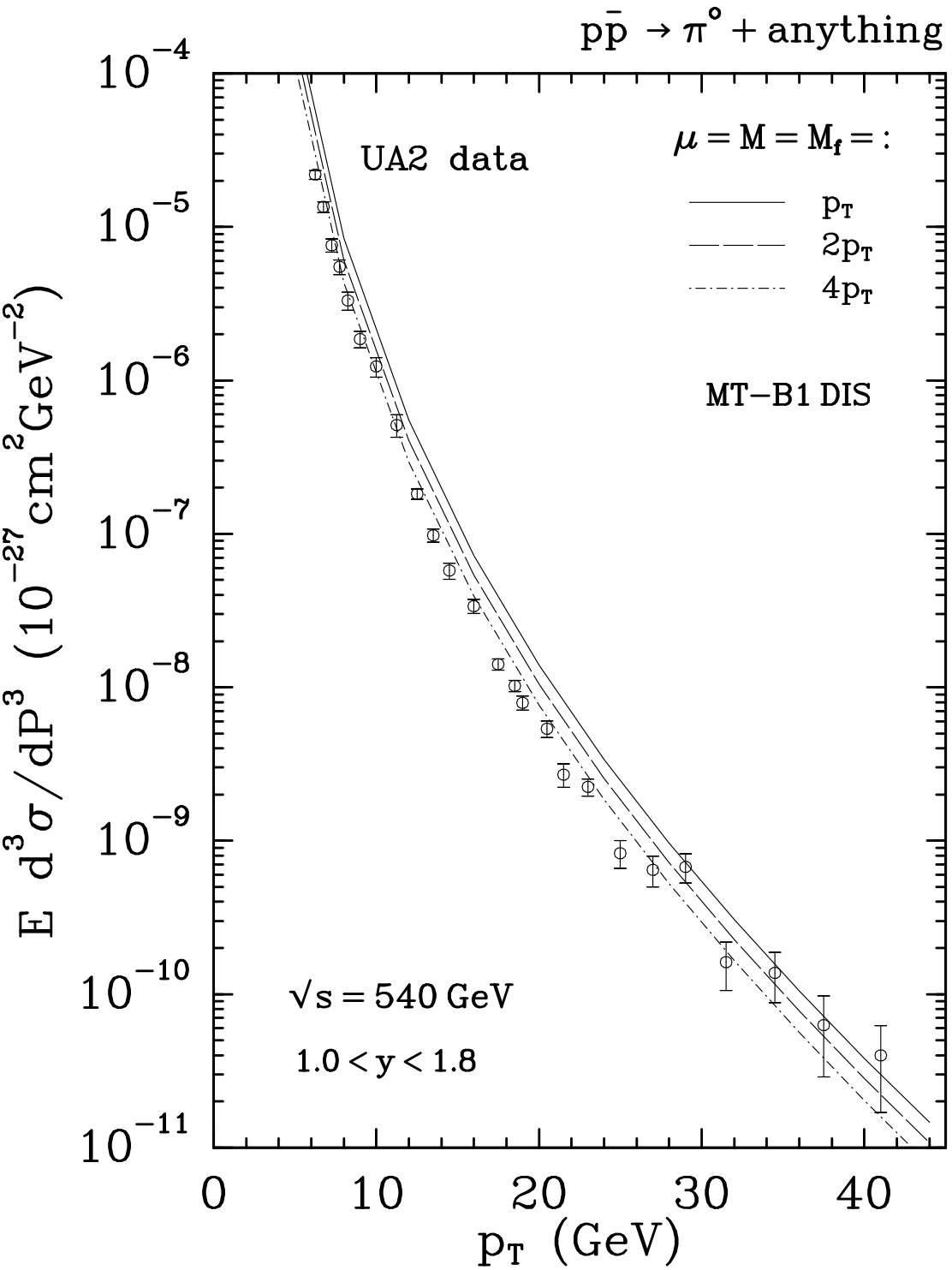

Figure 14: Inclusive π^0 production cross section for $\sqrt{s} = 540\,\text{GeV}$ averaged over the rapidity range $1.0 < y < 1.8$ compared to the experimental data obtained by the UA2 Collaboration. The short-dashed, solid and long-dashed lines correspond to the full NLO predictions for scales μ, M and M_f all set equal to p_T, $2p_\text{T}$ and $4p_\text{T}$, respectively.

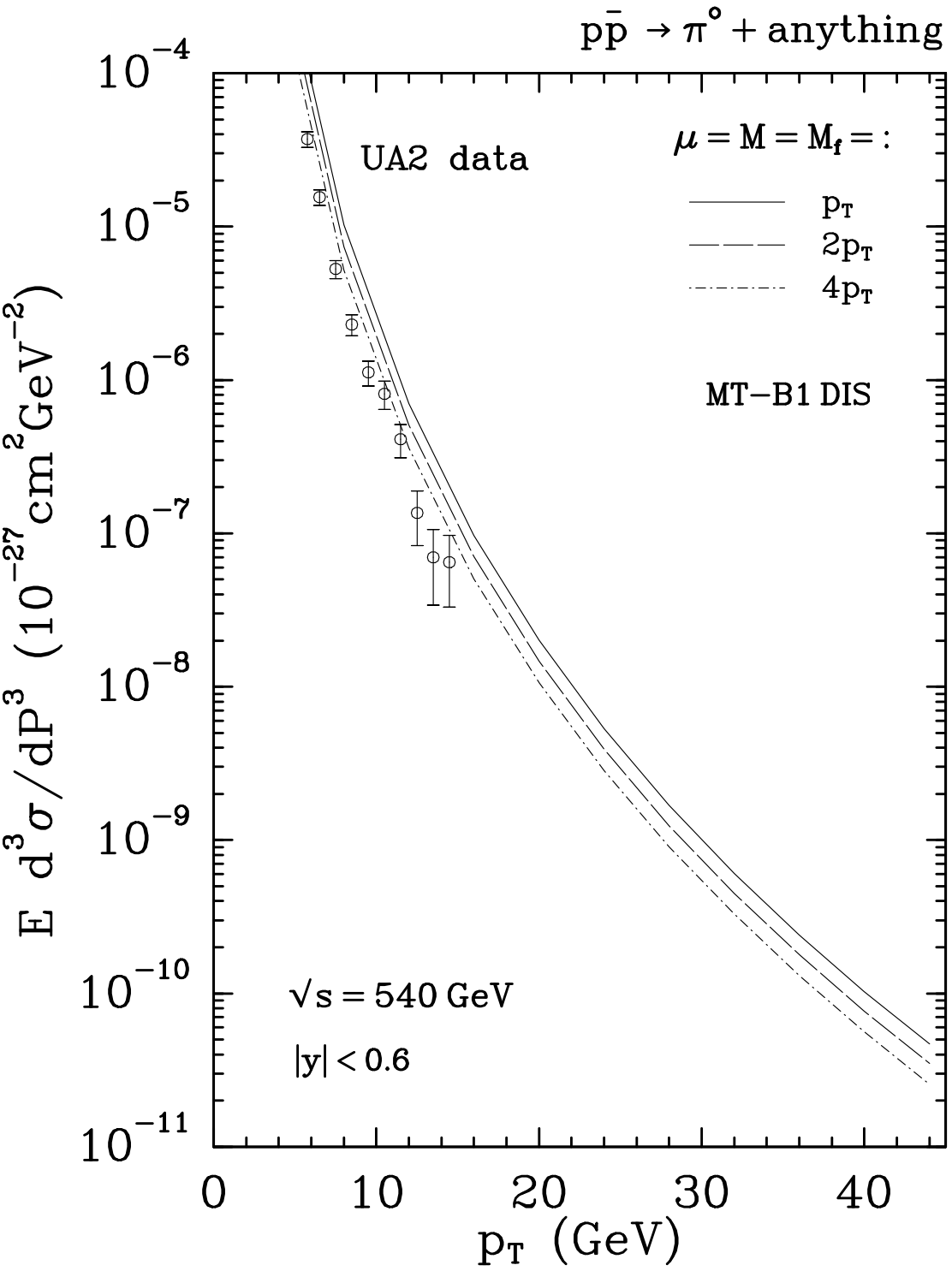

Figure 15: Same as in Fig. 14 for rapidity range $|y| < 1.0$.

definitely above the data. A reasonably good fit can be obtained only if we increase the value of these scales up to $4p_{\mathrm{T}}$. On the other hand, the fragmentation functions into π^0's might need to be revised, in particular the gluon fragmentation function, which is not much constrained by the e^+e^- data used in [4]. More work on the π^0 fragmentation functions is needed before a final conclusion concerning the scale appropriate to the π^0 production cross section can be drawn.

5 Summary and Conclusions

We have calculated inclusive single-charged-hadron and single-π^0 cross sections in NLO and compared our results with experimental data from the UA2 and CDF Collaborations. The overall agreement is satisfactory, surprisingly, also in the small-$p_{\rm T}$ region. At large $p_{\rm T}$, where QCD could be tested cleanly, experimental data are unfortunately rare and plagued by large errors. More accurate measurements in this region would obviously provide a better probe of the QCD predictions.

As expected, the scale dependence in NLO is reduced with respect to the one present in LO. Therefore, within the scale variation in NLO, our results can be considered as an absolute prediction for single-charged- and single-neutral-hadron production in $p\bar{p}$ collisions. The scale which yields the best agreement of the inclusive charged-hadron production cross section to the experimental data is equal to $p_{\rm T}$. Larger values, up to $4p_{\rm T}$, are needed to fit the data for inclusive π^0 production.

A drawback of our approach is that we still use fragmentation functions in LO. While this will be improved in the future when NLO fragmentation functions become available, we observe that already now the scale dependence of our results is reduced with respect to the one present in the LO calculation. We deduce that some compensation concerning the factorization scale M_f already works to a large extent.

When comparing our results to the LO ones with LO structure functions and one-loop $\alpha_{\rm S}$, we find that they roughly agree at scales just below $p_{\rm T}$. We consider this agreement as accidental, since they deviate from each other at different scales. The fact that the NLO hard scattering contributions are very important can be clearly seen when the NLO results are compared with the LO ones with $\alpha_{\rm S}$ and structure functions taken in NLO. In this case, for scales equal to $p_{\rm T}$, we find a K factor approximately 1.5.

We plan to extend this NLO approach to inclusive hadron production in γp and ep collisions. We expect in this case a somewhat different pattern due to the presence of the direct component in the photon structure function. Further work is also needed in the improvement of the fragmentation functions where a thorough analysis, similar to the one performed for the structure functions, is called for.

Acknowledgements We thank J.Ph. Guillet for providing the Fortran implementation of the results of [6] together with clarifying comments and S. Salesch for useful discussions. One of us (F.B.) thanks D. Michelsen and H. Spiesberger for advice on the phase space Monte Carlo integration and T. Ohl and M. Speh for support in using Emacs under HP-UX.

References

[1] J.C. Collins and D.E. Soper, *Ann. Rev. Nucl. Part. Sci.* **37** (1987) 383;
R. Baier, in *Nucleon-Nucleon and Nucleon-Antinucleon Interactions*, Proceedings of the XXIV. Internationale Universitätswochen für Kernphysik at Schladming, 1985, ed. by H. Mitter and W. Plessas (Springer-Verlag, Wien, 1985) p. 449;
J.C. Collins, D.E. Soper, and G. Sterman, in *Perturbative Quantum Chromodynamics*, ed. by A. Mueller (World Scientific, Singapore, 1989).

[2] J.F. Owens, *Rev. Mod. Phys.* **59** (1987) 465.

[3] B.L. Combridge, J. Kripfganz, and J. Ranft, *Phys. Lett.* **B70** (1977) 234;
R. Cutler and D. Sivers, *Phys. Rev.* **D17** (1978) 196;
R.P. Feynman, R.D. Field, and G.C. Fox, *Phys. Rev.* **D18** (1978) 3320.

[4] R. Baier, J. Engels, and B. Petersson, *Z. Phys.* **C2** (1979) 265.

[5] R.K. Ellis, M.A. Furman, H.E. Haber, and I. Hinchliffe, *Nucl. Phys.* **B173** (1980) 397.

[6] F. Aversa, P. Chiappetta, M. Greco, and J.Ph. Guillet, *Phys. Lett.* **B210** (1988) 225, *Phys. Lett.* **B211** (1988) 465 and *Nucl. Phys.* **B327** (1989) 105.

[7] J.G. Morfin and W.K. Tung, *Z. Phys.* **C52** (1991) 13.

[8] A.D. Martin, R.G. Roberts, and W.J. Stirling, *Phys. Rev.* **D37** (1988) 1161 and *Mod. Phys. Lett.* **A4** (1989) 1135;
P.N. Harriman, A.D. Martin, W.J. Stirling, and R.G. Roberts, *Phys. Rev.* **D42** (1990) 798;
J. Kwiecinski, A.D. Martin, W.J. Stirling, and R.G. Roberts, *Phys. Rev.* **D42** (1990) 3645.

[9] J.F. Owens and W.K. Tung, FERMILAB-PUB 92/59-T.

[10] G. Altarelli, R.K. Ellis, G. Martinelli, and S.-Y. Pi, *Nucl. Phys.* **B160** (1979) 301;
R. Baier and K. Fey, *Z. Phys.* **C2** (1979) 339.

[11] M. Anselmino, P. Kroll, and E. Leader, *Z. Phys.* **C18** (1983) 307.

[12] B. Alper et al., British-Scandinavian Collaboration, *Nucl. Phys.* **B87** (1975) 19 and *Nucl. Phys.* **B100** (1975) 237;
F.W. Büsser et al., *Nucl. Phys.* **B106** (1976) 1;
A.L.S. Angelis et al., CCOR Collaboration, *Phys. Lett.* **B79** (1978) 505;
D. Antreasyan et al., *Phys. Rev.* **D19** (1979) 764;
C. Kourkoumelis et al., *Z. Phys.* **C5** (1980) 95;
D. Drijard et al., CDHW Collaboration, *Nucl. Phys.* **B208** (1982) 1;
A. Breakstone et al., ABCDHW Collaboration, *Phys. Rev.* **D30** (1984) 528.

[13] J.D. Dowell, in *7th Topical Workshop on Proton-Antiproton Collider Physics*, FNAL, 1988, ed. by R. Raja, A. Tollestrup, and J. Yoh (World Scientific, Singapore, 1988) p. 115;
C. Albajar et al., UA1 Collaboration, *Nucl. Phys.* **B335** (1990) 261.

[14] M. Banner et al., UA2 Collaboration, *Phys. Lett.* **B122** (1983) 322 and *Z. Phys.* **C27** (1985) 329.

[15] A. Para, in *7th Topical Workshop on Proton-Antiproton Collider Physics*, FNAL, 1988, ed. by R. Raja, A. Tollestrup, and J. Yoh (World Scientific, Singapore, 1988) p. 131;
F. Abe et al., CDF Collaboration, *Phys. Rev. Lett.* **61** (1988) 1819.

[16] R.K. Ellis and J.C. Sexton, *Nucl. Phys.* **B269** (1986) 445.

[17] J.F. Owens, E. Reya, and M. Glück, *Phys. Rev.* **D18** (1978) 1501.

[18] K. Charchuła, *Comp. Phys. Commun.* **69** (1992) 360.

[19] B. Humpert, *Z. Phys.* **C27** (1985) 257.

[20] A.D. Martin, W.J. Stirling and R.G. Roberts, University of Durham preprint DTP/92/16, April 1992.

[21] E. Kabuss, Proceedings of DESY-Zeuthen Workshop on Deep Inelastic Scattering, April 1992;
S.R. Mishra et al., CCFR Collaboration, Columbia University preprint, NEVIS #1459, June 1992.

[22] G. Grunberg, *Phys. Lett.* **B95** (1980) 70 and *Phys. Rev.* **D28** (1984) 65.